68 Ga-radiolabeled AGuIX nanoparticles as dual-modality imaging agents for PET/MRI-guided radiation therapy

Penelope Bouziotis, Dimitris Stellas, Eloise Thomas, Charles Truillet, Charalampos Tsoukalas, François Lux, Theodoros Tsotakos, Stavros Xanthopoulos, Maria Paravatou-Petsotas, Anastasios Gaitanis, et al.

Research Article

For reprint orders, please contact: reprints@futuremedicine.com

Nanomedicine

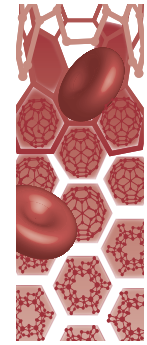

^{68}Ga-radiolabeled AGuIX nanoparticles as dual-modality imaging agents for PET/MRI-guided radiation therapy

Aim: The aim of this study was to develop a dual-modality positron emission tomography/magnetic resonance (PET/MR) imaging probe by radiolabeling gadolinium-containing AGuIX derivatives with the positron-emitter Gallium-68 (^{68}Ga). **Materials & methods:** AGuIX@NODAGA nanoparticles were labeled with ^{68}Ga at high efficiency. Tumor accumulation in an appropriate disease model was assessed by *ex vivo* biodistribution and *in vivo* PET/MR imaging. **Results:** ^{68}Ga-AGuIX@NODAGA was proven to passively accumulate in U87MG human glioblastoma tumor xenografts. Metabolite assessment in serum, urine and tumor samples showed that ^{68}Ga-AGuIX@NODAGA remains unmetabolized up to at least 60 min postinjection. **Conclusion:** This study demonstrates that ^{68}Ga-AGuIX@NODAGA can be used as a dual-modality PET/MR imaging agent with passive accumulation in the diseased area, thus showing great potential for PET/MR image-guided radiation therapy.

First draft submitted: 25 January 2017; Accepted for publication: 26 April 2017; Published online: 16 June 2017

Keywords: Gallium-68 • PET/MR imaging • ultrasmall AGuIX nanoparticles

Penelope Bouziotis*[,1], Dimitris Stellas[2], Eloïse Thomas[3], Charles Truillet[3], Charalampos Tsoukalas[1], François Lux[3], Theodoros Tsotakos[1], Stavros Xanthopoulos[1], Maria Paravatou-Petsotas[1], Anastasios Gaitanis[2], Lia Angela Moulopoulos[4], Vassilis Koutoulidis[4], Constantinos D Anagnostopoulos[2] & Olivier Tillement[3]

[1]Institute of Nuclear & Radiological Sciences & Technology, Energy & Safety, National Center for Scientific Research 'Demokritos', Aghia Paraskevi 15310, Athens, Greece

[2]Biomedical Research Foundation of the Academy of Athens, 4 Soranou Ephessiou Street, 11527, Athens, Greece

[3]Institut Lumière Matière, UMR5306 Université Lyon 1-CNRS, Université de Lyon, 69622 Villeurbanne cedex, France

[4]First Department of Radiology, School of Medicine, National & Kapodistrian University of Athens, 76 Vasilissis Sofias Avenue, 11528, Athens, Greece

*Author for correspondence: bouzioti@rrp.demokritos.gr

The development of multimodal imaging systems has led to a significant growth of dual-mode molecular imaging probes used for a range of different applications, including tumor imaging. Positron emission tomography/computed tomography (PET/CT) was introduced in clinical practice 15 years ago to enhance the strengths of the two modalities and minimize their limitations combining biological with anatomical information [1]. More recently, MRI has been used in place of CT to provide PET/MRI and SPECT/MRI hybrid imaging systems, capable of increased soft tissue contrast and resulting in lower radiation exposure [2]. Most of the multimodal agents developed to date have been combinations of either PET or MRI agents with optical agents. It is interesting to note that few SPECT/MRI and PET/MRI probes have been reported to this day but now, with the development of suitable equipment, there is a great scope for development of these kinds of probes. Dual-modality contrast agents, such as radiolabeled nanoparticles (NPs), are promising candidates for a number of diagnostic applications, since they combine the advantages of two different imaging modalities, namely PET imaging with MRI. The benefit of such a combination is to more accurately interpret disease and abnormalities *in vivo*, by exploiting the advantages of each imaging technique, in other words, high sensitivity for PET, high resolution anatomical information for MRI [3-6].

AGuIX NPs are ultrasmall rigid imaging NPs made of polysiloxane and surrounded by gadolinium chelates. They are obtained by a top-down process already described in the literature [7]. With a hydrodynamic diameter under 5 nm, they represent the first multifunctional silica-based NPs that are sufficiently small to escape hepatic clearance and enable animal imaging by four complemen-

Future Medicine part of fsg

tary techniques (MRI, SPECT after labelling by ^{111}In, fluorescence imaging and CT) [8]. Thanks to their radiosensitizing properties, AGuIX NPs have proven to be an excellent tool for radiation therapy, and recent literature shows how MRI can be used to perform image-guided radiation therapy with them [7,9-12]. However, a dual-modality PET/MRI imaging agent which combines the advantages of both imaging modalities has more to offer than a single-modality, gadolinium MR imaging agent, in this case, and can be used as a companion diagnostic agent.

Positron-emitting radionuclides, such as Fluorine-18, are produced at cyclotron facilities all over the world. An alternative production of positron-emitting radionuclides is via a generator system. Generators have the advantage of allowing clinical studies without an on-site cyclotron, thus providing radionuclides upon demand. Gallium-68 is one such radionuclide. The application of ^{68}Ga-labeled peptides has attracted considerable interest for cancer imaging because of its physical characteristics. ^{68}Ga decays at 89% through positron emission of 1.92 MeV (maximum energy) and can be eluted from an in-house ^{68}Ge/^{68}Ga generator (^{68}Ge, $T_{1/2}$ = 270.8 days), thus providing an ideal positron-emitting isotope without the need for an on-site cyclotron [13]. Furthermore, its physical half-life of 68 min renders it compatible with the *in vivo* pharmacokinetics of many peptides and antibody fragments. Thus, the application of ^{68}Ga-labeled peptides for cancer imaging has gained considerable interest in recent years [14,15]. One of the main advantages of ^{68}Ga is that it can be used as the diagnostic analogue of many trivalent radionuclides, for which the coordination chemistry is fully developed. In other words, the same chelator can be used for efficient labeling with the diagnostic radionuclide ^{68}Ga and with other therapeutic nuclides such as Yttrium-90 and Lutetium-177 [16].

Previous work from our group has shown that AGuIX derivatives labeled with ^{68}Ga are a promising imaging tool for simultaneous PET/MRI imaging [17]. The classical AGuIX NPs, made of polysiloxane and surrounded by DOTAGA(Gd^{3+}) covalently grafted to the inorganic matrix, have been modified in order to radiolabele them. While DOTA is a widely used chelator for gallium (log β = 13.7), NODAGA 2,2′-(7-(1-carboxy-4-((2,5-dioxopyrrolidin-1-yl)oxy)-4-oxobutyl)-1,4,7-triazanonane-1,4-diyl)diacetic acid) appears to be a more interesting chelate and has thus been grafted on the NPs for this labeling (log β = 30.98) [18]. *Ex vivo* biodistribution studies on normal mice showed an extremely low residual activity in all untargeted tissues, especially in organs where NPs are classically sequestered, such as the liver and lung (<2% ID/g at 120 min p.i.). These same NPs, functionalized with a desferrioxamine chelator instead of NODAGA, have also been labeled with Zirconium-89 for PET imaging applications [19]. By incorporating a long-lived isotope such as ^{89}Zr ($T_{1/2}$ = ~78 h) onto AGuIX, the amount of NPs at the cancerous site may be quantified at later time-points postinjection.

The present work aimed at showing that ^{68}Ga-AGuIX@NODAGA NPs can be used as dual-modality PET/MRI imaging agents capable of providing higher-quality, more detailed images for better planning of radiation therapy sessions. The objectives of the present study were to assess the passive accumulation of ^{68}Ga-AGuIX@NODAGA in a U87MG tumor model, both by *ex vivo* biodistribution studies and *in vivo* PET and MR imaging studies.

Materials & methods

All reagents and solvents were of chemical grade and used without further purification. Sodium hydroxide (NaOH, 99.99%), hydrochloric acid (HCl, 36.5–38%), dimethylsulfoxide (DMSO, >99.5%) and europium chloride hexahydrate ($EuCl_3$•6H2O, >99%) were purchased from Aldrich Chemical (France). Acetonitrile (CH_3CN, >99.9%) was purchased from Carlo Erba (France). Trifluoroacetic acid (TFA, >99%) was purchased from Alfa Aesar (United Kingdom). AGuIX particles were purchased from Nano-H/CheMatech (France). The derivative NODAGA-NHS chelate (2,2′-(7-(1-carboxy-4-((2,5-dioxopyrrolidin-1-yl)oxy)-4-oxobutyl)-1,4,7-triazonane-1,4-diyl)diacetic acid) was purchased from CheMatech (France). All products were used without further purification. Only Milli-Q water (ρ > 18 MΩ.cm) was used for the aqueous solution preparation. Elementary analysis of particles was performed by the Filab company (France).

HPLC was performed using a Waters 600 Controller pump, a Waters 996 Photodiode Array detector and a γ-RAM radioactivity detector to measure radioactive flow. The UV detection wavelength was 295 nm for all experiments. A lower activity commercial ^{68}Ge/^{68}Ga generator was acquired from Eckert & Ziegler (Berlin, Germany). HPLC analyses were performed on a Jupiter C4 column (150 × 4.60 mm, 5 µm, 300 Å, Phenomenex®, USA). The gradient systems used are given in the text. Solvents for HPLC were of analytical grade; before use they were filtered through 0.22 µm membrane filters (Millipore, MA, USA) and degassed. Radioactivity measurements were conducted in an automated well-typed γ-counter NaI(Tl) crystal (Packard). Tissue and blood samples were measured on a Packard COBRA II Auto-Gamma counter (Canberra, USA).

The U87MG cell line was acquired from ATCC (VA, USA). For cell culturing, Dulbecco's modified Eagle medium, fetal bovine serum, penicilline/streptomycin, L-glutamine and trypsin/EDTA solution were purchased from PAA Laboratories (GmbH, Austria). The bovine serum albumin, glutamax, HEPES, bacitracin, aprotinin and PMSF used were obtained from Sigma-Aldrich (GmbH, Austria).

Animals used for the biodistribution studies were obtained from the breeding facilities of the Institute of Biological Sciences, National Center for Scientific Research, Demokritos, Athens, Greece.

MRI studies were performed on a 1.5 Tesla MRI Unit (Philips Medical Systems, Best, The Netherlands).

PET scans were performed using a Mediso scanner (Mediso NanoScan PC, with 8 detector modules) with an axial field of view of 98.6 mm and a spatial resolution of 0.8 mm at the center of the scanner (with Tera-Tomo 3D PET iterative reconstruction). Prior to PET imaging, a CT scan was performed for attenuation correction and anatomic localization. The X-ray beam energy set at 50kVp, the exposure time at 300 msec and current at 670 µA. The number of projections per rotation was 480 and the slice thickness 250 µm. For the CT image reconstruction, a modified version of the Feldkamp algorithm and the Ram-Lak filter were used. PET and CT data were reconstructed using Nucline software version 2.01 (Build 011.0005). The PET image reconstruction was performed using a version of 3D OSEM algorithm (Tera-Tomo 3D PET image reconstruction algorithm) and voxel dimensions of 0.4 × 0.4 × 0.4 mm (size of image matrix 87 × 75 × 246). Dead time, decay, scatter, attenuation and axial sensitivity corrections as well as normalization were applied to PET data. Image analysis was performed with the Mediso InterView Fusion software package version 3.00.039.0000 BETA. Images were analyzed by drawing volumes of interests employing 'add isocount 3D Regions Of Interest (ROI)' option.

AGuIX@NODAGA synthesis

AGuIX NPs were synthesized according to an original top-down process already described in the literature [7] and presented briefly in the results part. They were then functionalized with NODAGA-NHS ((2,2′-(7-(1-carboxy-4-((2,5-dioxopyrrolidin-1-yl)oxy)-4-oxobutyl)-1,4,7-triazonane-1,4-diyl)diacetic acid). For this, 540 µmol of Gd of AGuIX were dispersed in 5.40 ml of water for 1 h at a pH of 7.1 ([Gd^{3+}] = 100 mM). Then 4.41 ml of water was added. 198 mg of the derivative NODAGA chelate (270 µmol; ratio Gd/DOTA = 2) was dissolved in 0.99 ml of DMSO ([NODAGA] = 200 mg/ml). This solution was then gradually added to the AGuIX solution under stirring at room temperature and the pH adjusted to 7.4 by addition of NaOH solution. The particles solution was stirred for 5 h 30 min.

AGuIX@NODAGA purification

The mixture was diluted in water to [Gd^{3+}] = 16.4 mM (V = 33 ml) in order to have a solution containing less than 4% DMSO and the pH decreased to 1 to avoid ionic interactions between ammonium of AGuIX and carboxylate of NODAGA-NHS. Particles were then purified by tangential filtration trough Vivaspin® membranes (MWCO = 5 kDa) purchased from Sartorius Stedim Biotech (France). The colloidal solution was introduced into Vivaspin tubes, and centrifuged. This step was repeated several times, by filling the tubes with water and centrifuging again, until the desired purification rate was reached (>25,000). The particles' solution was concentrated to approximately [Gd^{3+}] = 100 mM, the pH adjusted to 7.4 and finally the solution was sterile filtered through a 0.2 µm syringe filter in order to remove the largest impurities. It was freeze-dried for storage, using a Christ Alpha 1–2 lyophilisator. The Gd yield for the synthesis is 31%.

Radiolabeling of AGuIX@NODAGA NPs with ^{68}Ga

For the radiolabeling experiment, ^{68}Ga was eluted from the ^{68}Ge/^{68}Ga generator with 7 ml 0.1 N HCl and trapped onto an acidic cation exchange resin. Metal impurities (such as Zn, Fe, Ti and Ge) were removed by passage of 1 ml washing solution (N1, 80% acetone + 0.15 M HCl) [20]. Subsequent desorption of purified ^{68}Ga from the cation exchanger was afforded with 400 µl of 98% acetone and 2% 0.15 M HCl. For a typical preparation of ^{68}Ga-labeled AGuIX@NODAGA NPs, 50 µl AGuIX@NODAGA NPs (10 µmol [Gd^{3+}] in 200 µl H_2O) were mixed with 300 µl of sodium acetate buffer, pH 5.6 and 200 µl of ^{68}Ga eluate (50 MBq) were consequently added. The mixture was then vortexed and incubated for 20 min at 50–60°C. In order to determine the radiochemical purity of the labeled NPs, 10 µl aliquots of the reaction solution were analyzed by HPLC, applying a linear gradient system at a 1 ml/min flow rate from 0% B to 100% B in 20 min, where solvent A = 0.1% TFA in H_2O and solvent B = 0.1% TFA in AcCN. The radiolabeled complex was consequently purified on a PD10 column (GE Healthcare Bio-Sciences AB, Uppsala, Sweden) as follows. The PD10 column was first conditioned with 8 column volumes of phosphate-buffered saline (PBS) pH 7.4. The solution was then loaded onto the column, and ten 0.5 ml fractions were eluted with PBS. ^{68}Ga-AGuIX@NODAGA was first eluted as a yellowish suspension. The radioactivity of each frac-

tion was counted using an ionization chamber (Capintec Radioisotope Calibrator CRC-15, Capintec Inc., Ramsey USA). The fraction with the highest radioactivity was assessed for radiochemical purity by HPLC, as described above.

In vitro stability

In vitro stability of ^{68}Ga-AGuIX@NODAGA was assessed in serum for up to 3 h. For the labeling stability experiment, ^{68}Ga-AGuIX@NODAGA (0.4 MBq/100 µl) was incubated with 900 µl human serum in a 37°C water bath for 60, 120 and 180 min and then analyzed by ITLC-SG (mobile phase: 0.1 M citric acid). $^{68}Ga^{3+}$ is expected to move with the solvent front, while the labeled compound remains at the origin. All assays were performed in triplicate.

Animal model

Animal experiments were carried out according to European and national regulations. These studies have been further approved by our Institutional ethics committee and the procedures followed are in accordance with institutional guidelines. For experimental tumor models female SCID mice of 8 weeks on the day of inoculation were obtained from the breeding facilities of the Institute of Biology, NCSR 'Demokritos.' U87MG human glioblastoma cells (1×10^7 cells) were subcutaneously inoculated into the mice. The animals were housed in air-conditioned rooms under a 12-h light/dark cycle and allowed free access to food and water. Approximately 2 weeks after inoculation, *ex vivo* biodistribution studies and *in vivo* imaging studies on the tumor-bearing mice were performed.

Biodistribution studies

The *ex vivo* behavior of the radiolabeled compound was evaluated in athymic SCID mice (17–20 g) bearing U87MG glioblastoma tumors. Before injection in mice, a concentrated solution of AGuIX in water was added to ^{68}Ga-AGuIX@NODAGA, in order to obtain an injectable solution of 6.8 µmol [Gd^{3+}]/1 MBq (~6.8 mg NPs/100µl), which was administered via the tail vein. The biodistribution study was performed at 30, 60 and 120 min postinjection (n = 3 per time-point). Mice were sacrificed and the organs of interest, such as the heart, liver, kidneys, stomach, intestines, spleen, lungs, pancreas, bones and tumor were removed and together with samples of muscles and urine were weighed and counted in a NaI well counter (Packard COBRA II auto gamma counter). All measurements were corrected for background and radioactive decay. Tissue distribution data were calculated as the percent injected dose per gram (% ID/g), using an appropriate standard. Stomach and intestines were not emptied before the measurements. The% ID in whole blood was estimated assuming a whole-blood volume of 6.5% of the total body weight.

Metabolite studies

In urine, serum

Urine and blood metabolite assessment was performed at 15, 30 and 60 min p.i., in order to determine whether ^{68}Ga-AGuIX@NODAGA was metabolized after injection. Urine was collected at sacrifice time and centrifuged for 5 min at 2000 × *g* before RP-HPLC analysis. Blood collected from mice at the same time-points was also centrifuged for 10 min at 2000 × *g* and the supernatant (serum) was collected. Serum was treated with twice the volume of cold EtOH for protein precipitation. Samples were centrifuged at 2000 × *g* for 10 min. The remaining supernatant was separated and injected onto the HPLC column for analysis.

In tumor

Tumor samples were rapidly cut into small pieces and added to ice-cold PBS. Samples were homogenized, and the resulting homogenate was centrifuged (2000 r.p.m., 15 min). The supernatant was filtered through a 0.2 µm membrane before HPLC analysis, and 200 µl of the filtrate was directly injected onto the HPLC column. The conditions, acquisition and data processing were the same as described above for urine and serum.

In vivo imaging studies

PET imaging

To confirm the feasibility of using ^{68}Ga-AGuIX@NODAGA for passive tumor targeting, *in vivo* micro-PET scans were performed on a U87MG tumor model. U87MG mice were fasted for a period of 12 h prior to imaging. The PET studies were conducted using 2% isoflurane anesthesia in oxygen at 0.8 lt/min. The lateral tail vein of the mouse was injected with 6.7 MBq of ^{68}Ga-AGUIX@NODAGA in a volume of 150 µl (10.2 µmol [Gd^{3+}]/~10 mg NPs, as described above for *Biodistribution Studies*). Two different uptake times were tested: a 15 min uptake time followed by a 20 min static scan, and a 60 min uptake time followed by a 20 min static scan. During uptake time, the animal was anesthetized and its body temperature was maintained at 36°C on the scanner bed.

Histopathological studies

Two hours post-PET scanning, the mice were sacrificed and the tumors, the livers and the kidneys of each mouse were surgically removed. The tissues were then fixed in 10% formalin, embedded in paraffin, sectioned at 4 µm and stained with hematoxylin and eosin. The slides and the pictures of each tissue were

taken using an Olympus BX-50 microscope, equipped with an Olympus DP71 camera.

MR imaging

MRI exams were conducted at the Department of Radiology of the National and Kapodistrian University of Athens on a 1.5 Tesla unit (Philips Healthcare, Best, The Netherlands) using a surface phased-array coil. Anesthesia was induced with a mixture of ketamine/xylazine. T1-Weighted Turbo Spin Echo images were acquired before the injection of NPs. The next day mice were injected with AGuIX@NODAGA {20 µmol [Gd^{3+}] (~20 mg NPs/100 µl)} and were imaged 60 min postinjection with the same protocol. Signal intensity measurements were obtained on a dedicated workstation (Extended MR Workspace, Philips, Best, The Netherlands). Free-hand ROI were drawn around the tumors on the pre- and postinjection images. Care was taken to include as large a portion of the tumor as possible in the ROI.

Results

Synthesis & characterization of AGuIX NPs

AGuIX NPs were synthesized according to an original top-down process already described in the literature [7]. Briefly, gadolinium oxide core was synthesized in diethylene glycol before being encapsulated in a polysiloxane shell using hydrolysis-condensation of aminopropyltriethoxysilane (APTES) and tetraethylorthosilicate (TEOS). Thanks to the primary amino groups from APTES, the obtained nanostructures were then functionalized by DOTAGA chelates (1,4,7,10-tetraazacyclododecane-1-glutaric anhydride-4,7,10-triacetic acid). The NPs were then transferred from diethylene glycol to water leading to the core dissolution and the complexation of the Gd^{3+} ions by DOTAGA. The resulting polysiloxane hollow cores collapsed and fragmented into small and rigid platforms of polysiloxane: AGuIX NPs. AGuIX are therefore composed of a polysiloxane matrix surrounded by DOTAGA-Gd^{3+} and primary amino groups. AGuIX particles were then functionalized with the NODAGA-NHS (2,2′-(7-(1-carboxy-4-((2,5-dioxopyrrolidin-1-yl) oxy)-4-oxobutyl)-1,4,7-triazonane-1,4-diyl)diacetic acid) by incubating the chelate with particles in water, for 5 h 30 min at room temperature and at neutral pH. Thanks to the primary amines present at the surface of the particle, NODAGA was covalently grafted via an amide bond. The resulting AGuIX@NODAGA particles were purified by tangential filtration over a 5 kDa cut-off membrane. The purification was carried out at an acidic pH in order to avoid any ionic interactions that could occur between the amines of the particles and the carboxylic acids of the chelates.

AGuIX@NODAGA particles were characterized with several complementary technics (see Figure 1 & Supplementary Materials). They present a hydrodynamic diameter of 4.3 ± 0.9 nm suitable for renal excretion and closed to the one of AGuIX particles (3.6 ± 0.8 nm). The magnetic properties of AGuIX@NODAGA highlight their possible use as a positive contrast agent in MRI, indeed they present an r_1 = 16.7 s^{-1} mM^{-1} and an r_2/r_1 = 1.4 at 37°C and with a magnetic field of 1.4 T. The purity of AGuIX@NODAGA was checked by HPLC and the retention time determined. It is slightly higher than the one for AGuIX (13.9 and 12.6 min, respectively) which can be attributed to the modification of the particle surface.

The decrease of the isoelectric point (from 7.6 for AGuIX to 5.2 for AGuIX@NODAGA) is consistent with the functionalization and therefore the change of amino groups at the surface for carboxylic acids. In order to quantify more precisely the number of NODAGA grafted on particles, we performed a titration based on europium (Eu) luminescence [16,18]. When Eu^{3+} ions are not complexed and free in water, their luminescence is almost completely quenched by OH-oscillator. It is no more the case when Eu^{3+} ions are complexed by DOTAGA or NODAGA chelates. Indeed a signal at 592 nm is detected after an excitation at 395 nm. This difference was used to titrate available chelates at the NPs surface. Briefly, Eu^{3+} ions were added to a solution of AGuIX@NODAGA in water. They were complexed by NODAGA (and potential free DOTAGA) leading to an increase in the luminescence signal. When all the chelates have been saturated with Eu^{3+}, the luminescence reaches a plateau. Thanks to the change of slope we can determine the number of free chelates, available on the particles for radiolabeling. In our case, there are around 4.2 free chelates for 10 Gd (or one particle). The same experiment on AGuIX (data not shown) gives us 0.09 free DOTAGA for 10 Gd. Assuming there are no change in the number of free DOTAGA during the grafting of NODAGA, we can conclude that AGuIX@NODAGA particles present around 4.1 NODAGA for one particle. The same result was obtained, thanks to ICP-MS. Indeed, the following formula for AGuIX@NODAGA can be proposed: $Gd_{10}APTES^*_{33}TEOS^*_{41}DOTAGA^*_{10.2}NODAGA^*_{4.1}$.

Radiolabeling & *in vitro* stability assessment

AGuIX NPs bearing NODAGA (AGuIX@NODAGA) were radiolabeled with ^{68}Ga eluate after 20 min heating at approximately 50°C, and were subjected to RP-HPLC analysis. The chromatogram showed a minor peak at approximately 2.5 min, corresponding to uncomplexed ^{68}Ga (~15%), as well as a major peak

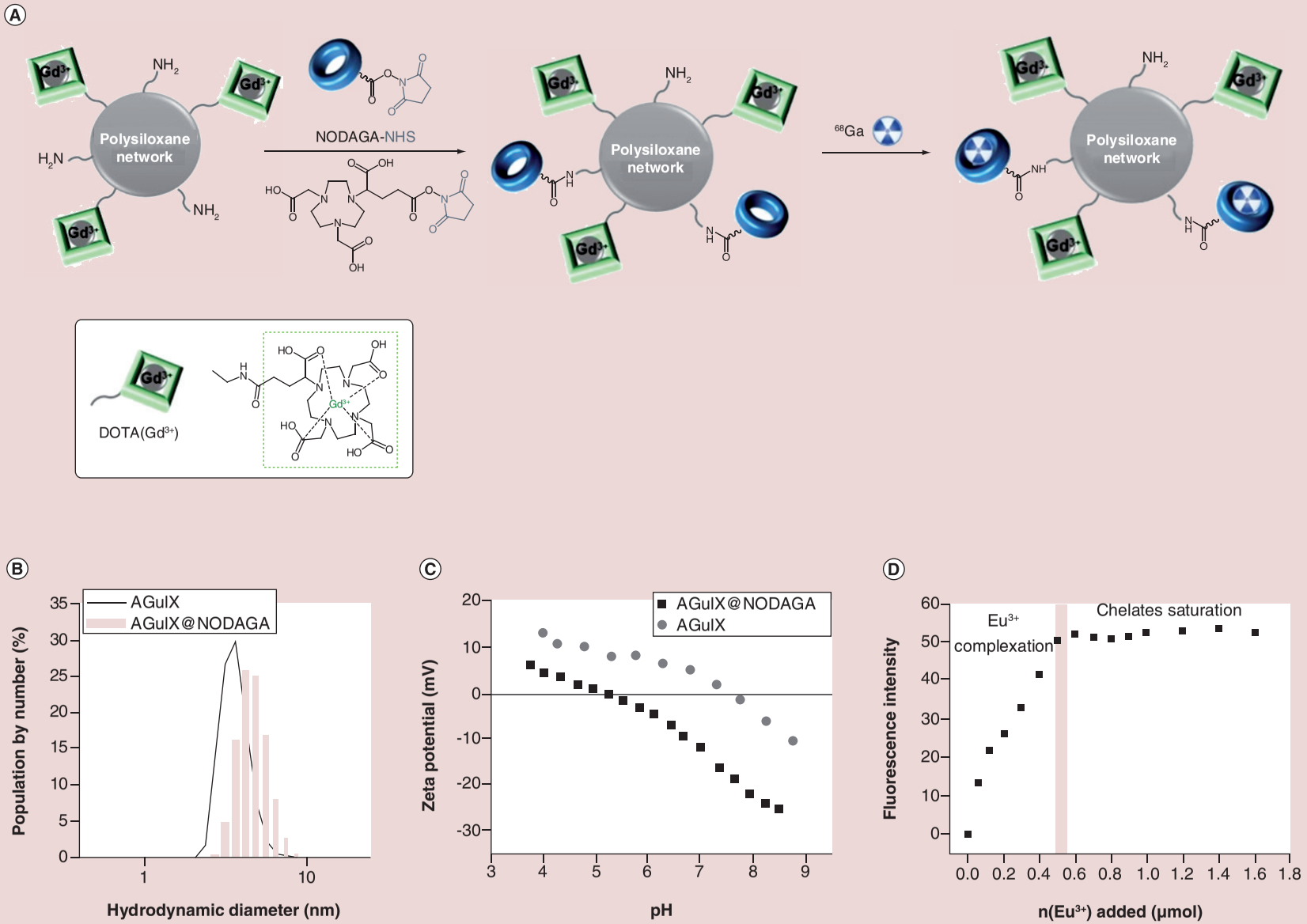

Figure 1. AGuIX@NODAGA synthesis and characterization. **(A)** Functionalization of AGuIX NPs with NODAGA and radiolabeling of the obtained AGuIX@NODAGA particles with ^{68}Ga. **(B)** Dynamic light scattering data showing the hydrodynamic diameter of AGuIX@NODAGA and AGuIX particles. **(C)** Evolution of the Zeta potential of AGuIX and AGuIX@NODAGA with pH. The isoelectric point for AGuIX@NODAGA is smaller than the one for AGuIX as expected. **(D)** Titration of available chelates on AGuIX@NODAGA thanks to europium luminescence. n_{Gd3+} = 1.2 µmol. Excitation wavelength: 395 nm. Emission wavelength: 592 nm.

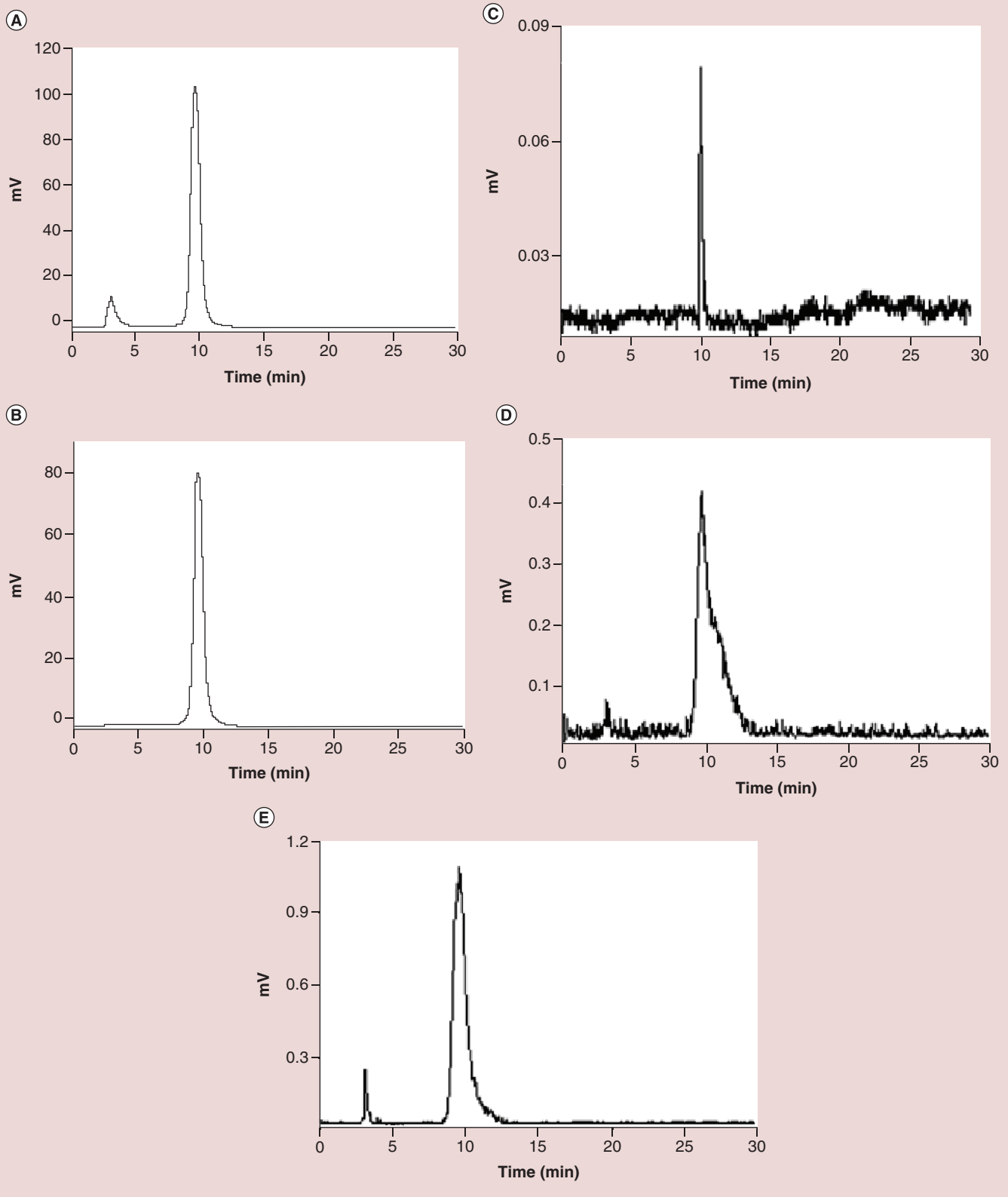

Figure 2. Metabolite studies of ^{68}Ga-AGuIX@NODAGA in tumor (C), blood (D) and urine (E) of tumor-bearing mice, at 60 min postinjection (the pre- and postpurification high performance liquid chromatography curves, (A) and (B) respectively, are given as a reference).

at approximately 10 min, which is attributed to ^{68}Ga-AGuIX@NODAGA (~85%) (Figure 2A). Extended heating was shown not to improve the radiolabeling yield. Therefore, ^{68}Ga-AGuIX@NODAGA was subjected to purification on a PD10 column, using PBS pH 7.4 as the eluent. HPLC assessment of the purified ^{68}Ga-AGuIX showed a single peak at approximately 10 min, with practically no evidence of free ^{68}Ga (RCP > 99%, Figure 2B). The radiolabeled complex was stable in saline at RT up to 3 h.

Serum stability testing shows how well a radiotracer is tolerated *in vivo*. ^{68}Ga should remain coordinated to AGuIX@NODAGA and not released into the bloodstream. Serum stability assessment up to 3 h at 37°C showed that the complex remained almost completely intact after a 3 h incubation period (over 98% retention of the radiolabel). Further assessment was not possible, due to the short half-life of ^{68}Ga.

In vivo stability, biodistribution & imaging studies

The next step of our studies involved the assessment of the metabolite profile of ^{68}Ga-AGuIX@NODAGA in mouse blood and urine, as well as in tumor tissue, of a U87MG subcutaneous tumor model. As demonstrated by HPLC analysis of tumor samples, a single peak corresponding to the peak for ^{68}Ga-AGuIX@NODAGA was also observed, with no other radioactive components present, suggesting that the radioactivity detected in the tumor samples is entirely attributable to unmetabolized ^{68}Ga-AGuIX@NODAGA (Figure 2C). In mouse blood and urine samples at 15, 30 and 60 min postinjection of the radiotracer, no evidence of degradation of ^{68}Ga-AGuIX@NODAGA was observed in all cases for blood, while for urine the amount of intact radiolabeled AGuIX@NODAGA was between 90 and 95% (Figure 2D & E, respectively). This may be attributed to small NP fragments containing ^{68}Ga-NODAGA.

Biodistribution and imaging studies followed in U87MG tumor-bearing mice injected with ^{68}Ga-AGuIX@NODAGA via the tail vein. *Ex vivo* biodistribution was investigated at 30, 60 and 120 min postinjection (Figure 3 & Supplementary Table 1) and showed that the radiotracer passively accumulated in the tumor at 30 min p.i. (1.03 ± 0.11% ID/g) and remains practically stable at 60 min p.i. (1.10 ± 0.16% ID/g). The excretion route was primarily via the urinary tract, as no significant liver or intestinal uptake was observed. Apart from the kidneys and blood, no major uptake in all analyzed tissues is noted (<1.5% ID/g from 30 min p.i.). These results are in accordance to *ex vivo* biodistribution studies previously performed in normal Swiss mice, which showed that ^{68}Ga-AGuIX@NODAGA cleared rapidly from the blood via the kidneys to the urine, resulting in extremely low background activity in all other tissues [17]. While the actual tumor uptake dropped from 30 to 120 min p.i., the Tumor/Blood and Tumor/Muscle (T/M) ratios increased over time, with the T/M ratio reaching a value of almost 5 at 120 min p.i., suggesting a clear differentiation between the affected and nonaffected tissue (Figure 4 & Supplementary Table 1).

After evidence of tumor accumulation was provided by the *ex vivo* biodistribution study, PET and MR imaging were performed on U87MG tumor-bearing SCID mice. By comparing MR images of mice before and after injection with AGuIX@NODAGA,

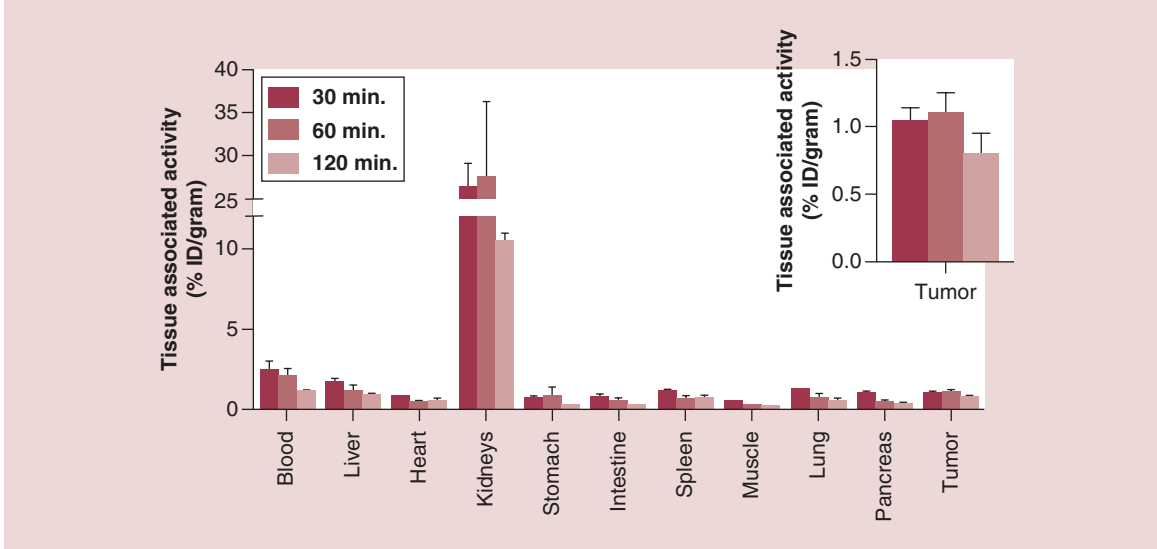

Figure 3. Biodistribution of ^{68}Ga-AGuIX@NODAGA in U87MG tumor-bearing mice.

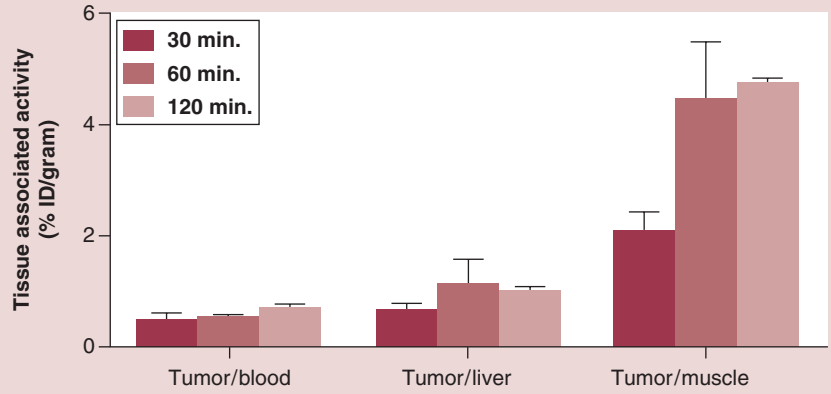

Figure 4. Tumor-to-tissue ratios ^{68}Ga-AGuIX@NODAGA at 30, 60 and 120 min postinjection.

we observed positive contrast at 60 min postinjection of the Gd-bearing AGuIX@NODAGA (Figure 5). The PET image of mice injected with ^{68}Ga-AGuIX@NODAGA showed accumulation of the radiotracer in the tumor from 15 min p.i., which was retained at the tumor site up to 60 min p.i. (Figure 6). Further *in vivo* assessment on the PET camera was not possible, due to the short half-life of ^{68}Ga.

Histology studies

Finally, histopathology studies showed that unmetabolized ^{68}Ga-AGuIX@NODAGA NPs are passively accumulated into the tumor, as depicted in Figure 7, frames (E) and (F). The histopathological features of the livers of the examined animals showed no, or scarce evidence of the NPs accumulated into the liver (Figure 7G). On the contrary, the kidneys at that time point were already full of urine containing the aforementioned NPs (Figure 7H).

Discussion

The design of the AGuIX NPs has been made in order to ensure a fast and exclusive renal elimination and to avoid toxicity concerns [9,12,21,22]. The present work was designed to assess the passive accumulation of ^{68}Ga-AGuIX@NODAGA in a U87MG tumor model, both by *ex vivo* biodistribution studies and *in vivo* PET and MR imaging studies.

Radiolabeling of AGuIX@NODAGA with the positron-emitter ^{68}Ga afforded a product of more than 99% radiochemical purity after purification, which is stable for at least 60 min p.i., and which accumulates in subcutaneous U87MG tumors. Tumor uptake peaked at 1 h p.i. (1.10 ± 0.16% ID/g), while the T/M ratio increased over time, reaching a value of almost 5 at 120 min p.i. This provides us with ample time for PET/MR visualization of these areas, as early imaging has been shown to be promising for precise tumor delineation, as previously demonstrated [23,24]. Furthermore it was shown that no radiolabeled derivatives of the parent radiotracer were detected in samples of serum, urine and tumor tissue, thus associating the biodistribution data entirely with the uptake of intact ^{68}Ga-AGuIX@NODAGA.

One of the most significant advantages of PET is its sensitivity and its ability to be quantified. PET imaging tracers injected at very low concentrations are sufficient to provide high-quality images [25,26]. This fact was our first steppingstone for the initiation of our experiments to go as low as possible, in other words, to achieve a high specific activity product to work with. However, this approach would prove to be problematic in the case of a dual-modality PET/MR imaging agent, since MR imaging requires much higher concentrations of injected contrast agent, in order to provide satisfactory images. We finally opted to work with AGuIX@NODAGA samples having an adequately high concen-

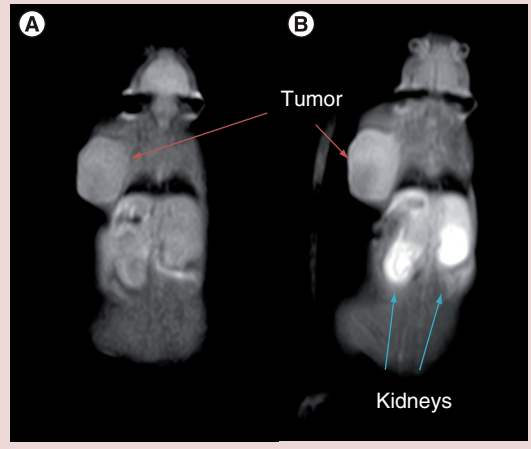

Figure 5. T1-weighted magnetic resonance images of a U87MG tumor-bearing mouse before (A) and 60 min after (B) injection of 20 μmol AGuIX@NODAGA.

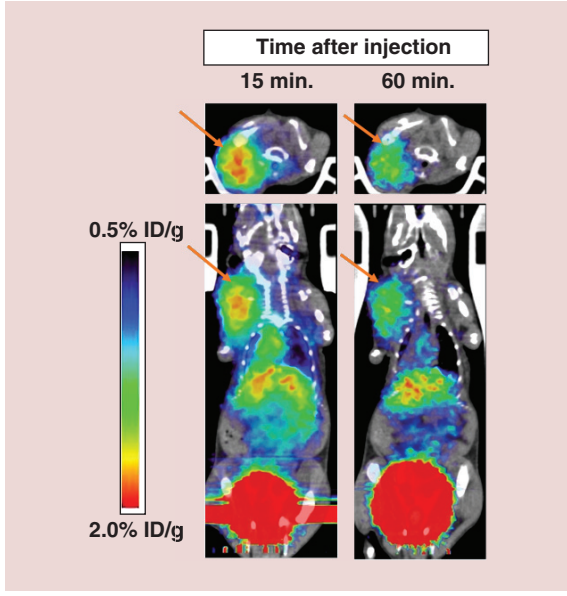

Figure 6. Positron emission tomography image of a U87MG tumor-bearing mouse injected with ^{68}Ga-AGuIX@NODAGA, at 30 and 60 min p.i.

tration for satisfactory MR imaging, and to adjust the amount of radioisotope to provide an imaging tracer for simultaneous PET/MR imaging. The PET signal permits the precise quantification of the concentration of NPs in tumors for future treatments, using the radiosensitizing properties of AGuIX.

Radiolabeling of a low concentration AGuIX@NODAGA sample (500 nmol [Gd^{3+}]/~500 µg NPs/100 µl) with ^{68}Ga was easily accomplished and stability of the radiolabeled product was shown. For comparison, a high-concentration ^{68}Ga-AGuIX@NODAGA sample (6.8 µmol [Gd^{3+}]/~6.8 mg NPs/100 µl) was prepared, at a NP concentration similar to that required for MRI imaging (due to Gd). *Ex vivo* biodistribution studies on tumor-bearing mice with both low- and high-concentration samples (500 nmol/100 µl vs 6.8 µmol/100 µl) showed tumor uptake for both samples, however fast washout from the tumor was observed for the low-concentration product. This can be explained by the increased biodegradability of the NP at high dilution because of the Si–O–Si bond hydrolysis. For concentrated solutions of AGuIX, no degradation occurs. The NPs are accumulated in the tumors and it seems like a local increase of the concentration of the NPs in the tumors occurs. *In vitro* experiments previously published by the team on accumulation in tumors have shown that the NPs are internalized in tumors cells notably by macropinocytosis mechanism [27]. In the vesicles, the NPs are aggregated. In the tumor environment, a similar aggregation can occur that can explain the nondegradation of the NPs observed in the tumor. The results presented here show moderate tumor accumulation via passive targeting, which are comparable to results described by other groups in the literature [28-31]. However, while tumor uptake is quite similar, uptake in the RES organs is much higher in those studies, which could be problematic for future clinical translation.

We next focused on the metabolite study of the injected ^{68}Ga-AGuIX@NODAGA, in order to see how these two different concentrations of radiotracer behave *in vivo*.

In general, for successful translation of a radiolabeled imaging agent to the clinical, it is very important to evaluate the degree to which the association between the radioactive label and the core molecule remains intact *in vivo* [25,32]. In our case, it is critical to assess the stability of radiolabeled NPs, once administered into systemic circulation. One of the objectives of this work was to study the *in vivo* integrity of AGuIX@NODAGA NPs labeled with ^{68}Ga.

Metabolite studies were performed on blood, urine and tumor samples taken from U87MG tumor-bearing SCID mice injected with ^{68}Ga-AGuIX@NODAGA. Our evaluation showed that the high specific activity product (i.e., radiolabeling of a low-concentration AGuIX@NODAGA sample, 500 nmol [Gd^{3+}]/~500 µg NPs/100 µl) was rapidly degraded (>90% degradation at 5 min p.i., data not shown). On the other hand, the high-concentration ^{68}Ga-AGuIX@NODAGA sample (6.8 µmol [Gd^{3+}]/~6.8 mg NPs/100 µl) was metabolically stable up to 60 min p.i., in all evaluated samples. This result perfectly suits our needs for a dual-modality imaging agent, administered at concentrations adequate for both PET and MRI imaging modalities, as was proven by imaging studies that followed.

PET imaging of the low concentration AGuIX@NODAGA sample (500 nmol [Gd^{3+}]/~500 µg NPs/100 µl) showed rapid tumor uptake up to 10 min p.i., with consequent, washout from the tumor site (data not shown). This is in accordance with our metabolite studies discussed above. When a high concentration radiolabeled sample was injected into the tumor-bearing mice (6.8 µmol [Gd^{3+}]/~6.8 mg NPs/100 µl, 150 µl injected sample), the tumor could be clearly delineated up to 60 min p.i. (Figure 5). MR images acquired after administration of AGuIX@NODAGA NPs at a similar concentration gave excellent images with a significant positive contrast.

As toxicity is always a major concern with gadolinium-based MRI contrast agents, Sancey *et al.* evaluated the maximum tolerated dose of AGuIX NPs [22]. For *in vivo* application in mice, it was proven that after bolus injection of these NPs, no toxicity effects were shown at doses up to ten-times higher than the ther-

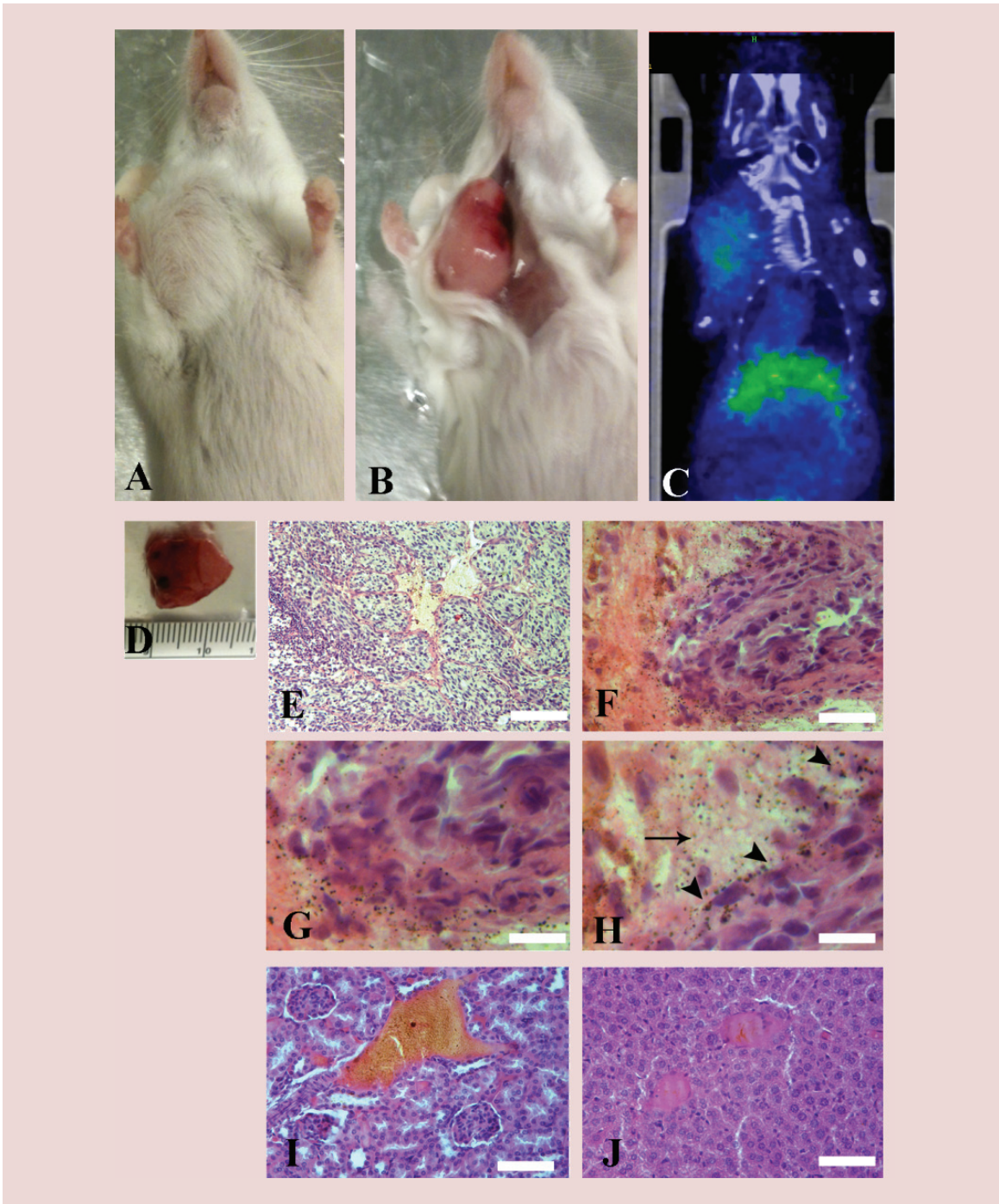

Figure 7. Histopathological studies. **(A & B)** Gross anatomic features of ^{68}Ga-AGuIX@NODAGA injected mouse post mortem. **(C)** Positron emission tomography/computed tomography overlay image verifies the accumulation of ^{68}Ga-AGuIX@NODAGA nanoparticles (NPs) in the tumor. ^{68}Ga-AGuIX@NODAGA NPs are also weakly present in the liver. **(D)** The gross anatomy of the U87MG generated tumor after the excision. **(E & F)** Low magnification (scale bar = 200 μm) and high magnification (scale bar = 100 μm) of the U87MG tumor stained with Hematoxylin and Eosin. It is noteworthy that the ^{68}Ga-AGuIX@NODAGA NPs are trapped inside the tumor parenchyma, especially in areas where necrotic features are more evident. **(G & H)** Higher magnification of the U87MG tumor. With an arrow we indicate the necrotic area and with arrowheads the location of the NPs (scale bar = 25 μm). **(I)** The high magnification of a section of the kidney counterstained with H&E also verifies the minor accumulation of ^{68}Ga-AGuIX@NODAGA NPs as detected with the micro-PET camera (scale bar = 100 μm). **(J)** The high magnification of a section of the liver counterstained with H&E verifies the minor accumulation of ^{68}Ga-AGuIX@NODAGA NPs as detected with the micro-PET camera (scale bar = 100 μm).

apeutic dose, which corresponds to an injection of 8 µmol of [Gd^{3+}]. Furthermore, no significant difference in creatinine levels between AGuIX and control groups was recorded, suggesting the absence of any significant nephrotoxicity related to AGuIX NPs [9].

The ultrasmall size of the AGuIX leading to rapid elimination indeed limits circulating time in the blood but it seems like it permits a better penetration in tumors, as emphasized by recent papers which compare different size of NPs and their ability to penetrate into the tumor and to leave the perivascular space [33]. The interest of the active targeting for nanomedicine is still controversial [34,35]. For receptors present on the membrane of the tumor cells, the NPs have to be firstly accumulated in tumors by EPR effect and so active targeting will probably not drastically increase the quantity of NPs accumulated in the tumor (factor 2 or 3), as we have shown in precedent papers [36]. However, it will probably increase the retention time in the tumor and so be interesting for further theranostic applications.

Conclusion

In conclusion, we have developed NODAGA-functionalized AGuIX NPs, and then efficiently labeled them with the positron emitter Ga-68. We have evaluated the integrity of these radiolabeled NPs in the mouse and have reached the conclusion that ^{68}Ga-AGuIX@NODAGA, when injected at a concentration which was appropriately tailored to the sensitivity of both PET and MR imaging modalities, remains unmetabolized in the mouse, thus providing a single-injection, dual-modality imaging agent adequate for both PET and MR imaging. *Ex vivo* biodistribution and *in vivo* PET and MR imaging studies provide further evidence of this. Second-generation AGuIX NPs will be developed, which will be functionalized for active targeting.

Future perspective

^{68}Ga-AGuIX@NODAGA NPs show promising properties as a dual-modality imaging agent and exhibit great potential for PET/MR image-guided radiation therapy of cancer.

Financial & competing interests disclosure

The authors acknowledge financial support from the French National Research Agency (ANR6126RPIB-0010 Multimage). François Lux and Olivier Tillement have one patent to disclose: WO2011135101. This patent protects some of the nanoparticles described in this publication: AGuIX. The authors have no other relevant affiliations or financial involvement with any organization or entity with a financial interest in or financial conflict with the subject matter or materials discussed in the manuscript apart from those disclosed.

No writing assistance was utilized in the production of this manuscript.

Summary points

Objectives

- To assess the passive accumulation of ^{68}Ga-AGuIX@NODAGA in a U87MG tumor model, both by *ex vivo* biodistribution studies and *in vivo* PET and MR imaging studies.

Results

- AGuIX nanoparticles (NPs) were functionalized with the NODAGA-NHS (2,2′-(7-(1-carboxy-4-((2,5-dioxopyrrolidin-1-yl)oxy)-4-oxobutyl)-1,4,7-triazonane-1,4-diyl)diacetic acid). AGuIX@NODAGA particles present around 4.1 NODAGA for one particle.
- AGuIX@NODAGA NPs were radiolabeled with ^{68}Ga (radiochemical purity >99% after purification).
- The radiolabeled complex was stable in saline at RT up to 3 h. Serum stability assessment up to 3 h at 37°C showed that the complex remained almost completely intact after a 3 h incubation period.
- Metabolite analysis showed no evidence of degradation of ^{68}Ga-AGuIX in blood, while for urine the amount of intact radiolabeled AGuIX was between 90 and 95%. In tumor samples, a single peak corresponding to the peak for ^{68}Ga-AGuIX@NODAGA was observed, suggesting that the radioactivity detected in the tumor samples is entirely attributable to unmetabolized ^{68}Ga-AGuIX@NODAGA.
- *Ex vivo* biodistribution showed that the radiotracer passively accumulated in the tumor. The excretion route was primarily via the urinary tract, as no significant liver or intestinal uptake was observed.
- Tumor/Blood and Tumor/Muscle ratios increased over time, thus providing a clear differentiation between the affected and nonaffected tissue.
- PET and MR imaging showed accumulation of the radiotracer in the tumor up to 60 min p.i.
- Histopathology studies showed that un-metabolized ^{68}Ga-AGuIX@NODAGA NPs are passively accumulated into the tumor.

Conclusion

- This study includes the first investigation of ^{68}Ga-AGuIX@NODAGA as a single-injection, dual-modality PET/MR imaging agent, which can improve diagnostic performance for cancer detection. As a result of this, they exhibit great potential for PET/MR image-guided radiation therapy.

Acknowledgements

Acknowledgements are due to Professor Frank Roesch and Professor Helmut R. Maecke, for provision of the ^{68}Ge/^{68}Ga generators utilized in this work, and for their valuable expertise in ^{68}Ga chemistry.

Ethical conduct of research

The authors state that they have obtained appropriate institutional review board approval or have followed the principles outlined in the Declaration of Helsinki for all human or animal experimental investigations. In addition, for investigations involving human subjects, informed consent has been obtained from the participants involved.

References

Papers of special note have been highlighted as: • of interest; •• of considerable interest

1 Griffeth LK. Use of PET/CT scanning in cancer patients: technical and practical considerations. *BUMC Proceedings* 18, 321–330 (2005).

2 Drzezga A, Souvatzoglou M, Eiber M *et al.* First clinical experience with integrated whole-body PET/MR: comparison to PET/CT in patients with oncological diagnoses. *J. Nucl. Med.* 53, 845–855 (2012).

3 Kim SA, Kim Y-H, Kim JH *et al.* Development and *in vivo* imaging of a PET/MRI nanoprobe with enhanced NIR fluorescence by dye encapsulation. *Nanomedicine* 7, 219–229 (2012).

4 Lee H-Y, Li Z, Chen K *et al.* PET/MRI dual-modality tumor imaging using arginine-glycine-aspartic (RGD)-conjugated radiolabeled iron oxide nanoparticles. *J. Nucl. Med.* 49, 1371–1379 (2008).

5 Yang X, Hong H, Grailer JJ *et al.* cRGD-functionalized, DOX-conjugated, and ^{64}Cu-labeled superparamagnetic iron oxide nanoparticles for targeted anticancer drug delivery and PET/MR imaging. *Biomaterials* 32, 4151–4160 (2011).

6 Tsoukalas C, Laurent G, Sanchez GJ *et al.* Initial in vitro and in vivo assessment of Au@DTDTPA-RGD nanoparticles for Gd-MRI and ^{68}Ga-PET dual-modality imaging. *EJNMMI Phys.* 2, A89 (2015).

7 De Luc G, Roux S, Paruta-Tuarez A *et al.* Advantages of gadolinium based ultrasmall nanoparticles vs molecular gadolinium chelates for radiotherapy guided by MRI for glioma treatment. *Cancer Nanotechnol.* 5, 4 (2014).

• **AGuIX NPs versus gadolinium-based molecular agent: comparison of their efficiency for MRI and radiosensitization.**

8 Lux F, Mignot A, Mowat P *et al.* Ultrasmall rigid particles as multimodal probes for medical applications. *Angew. Chem. Int. Ed. Engl.* 50(51), 12299–12303 (2011).

•• **First report on the synthesis and characterization of ultrasmall AGuIX nanoparticles (NPs).**

9 Sancey L, Lux F, Kotb S *et al.* The use of theranostic gadolinium-based nanoprobes to improve radiotherapy efficacy. *Br. J. Radiol.* 87, 20140134 (2014).

•• **Review demonstrating that gadolinium-based NPs, in particular AGuIX, hold significant potential as theranostic agents.**

10 Dufort S, Le Duc G, Salomé M *et al.* The high radiosensitizing efficiency of a trace of gadolinium-based nanoparticles in the tumor. *Sci. Rep.* 6, 29678, (2016).

11 Dufort S, Bianchi A, Henry M *et al.* Nebulized gadolinium-based nanoparticles: a theranostic approach for lung tumor imaging and radiosensitization. *Small* 11, 215–221 (2015).

12 Lux F, Sancey L, Bianchi A *et al.* Gadolinium-based nanoparticles for theranostic MRI-radiosensitization. *Nanomedicine* 10(11), 1801–1805 (2015).

•• **Interesting review on gadolinium NPs for biomedical applications, in particular for MR image-guided radiotherapy.**

13 Fani M, Andre JP, Maecke HR. ^{68}Ga-PET: a powerful generator-based alternative to cyclotron-based PET radiopharmaceuticals. *Contrast Media Mol. Imaging* 3, 53–63 (2008).

14 Al-Nahhas A, Fanti S. Radiolabelled peptides in diagnosis and therapy: an introduction. *Eur. J. Nucl. Med. Mol. Imaging* 39(Suppl. 1), S1–S3 (2012).

15 Decristoforo C, Pickett RD, Verbruggen A. Feasibility and availability of ^{68}Ga-labelled peptides. *Eur. J. Nucl. Med. Mol. Imaging* 39(Suppl. 1), S31–S40 (2012).

16 Roesch F, Baum RP. Generator-based PET radiopharmaceuticals for molecular imaging of tumours: on the way to THERANOSTICS. *Dalton Trans.* 40(23), 6104–6112 (2011).

17 Truillet C, Bouziotis P, Tsoukalas C *et al.* Ultrasmall particles for Gd-MRI and ^{68}Ga-PET dual imaging. *Contrast Media Mol. Imaging* 10(4), 309–19 (2015).

•• **First report on the radiolabeling of AGuIX NPs with Gallium-68.**

18 Mignot A, Truillet C, Lux F *et al.* A top-down synthesis route to ultrasmall multifunctional Gd-based silica nanoparticles for theranostic applications. *Chemistry* 19(19), 6122–6136 (2013).

19 Truillet C, Thomas E, Lux F *et al.* Synthesis and characterization of ^{89}Zr-labeled ultrasmall nanoparticles. *Mol. Pharm.* 13, 2596–2601 (2016).

• **First report on a Zirconium-labeled ultrasmall NP.**

20 Zhernosekov KP, Filosofov DV, Baum RP *et al.* Processing of generator-produced ^{68}Ga for medical application. *J. Nucl. Med.* 48, 1741–1748 (2007).

21 Detappe A, Kunjachan S, Sancey L *et al.* Advanced multimodal nanoparticles delay tumor progression with

clinical radiation therapy. *J. Control. Release* 238, 103–113 (2016).

22 Sancey L, Kotb S, Truillet C *et al.* Long-term in vivo clearance of gadolinium-based AGuIX nanoparticles and their biocompatibility after systemic injection. *ACS Nano* 9(13), 2477–2488 (2015).

23 Le Duc G, Miladi I, Alric C *et al.* Toward and image-guided microbeam radiation therapy using gadolinium-based nanoparticles. *ACS Nano* 5(12), 9566–9574 (2011).

24 Bianchi A, Dufort S, Lux F *et al.* Targeting and *in vivo* imaging of non-small-cell lung cancer using nebulized multimodal contrast agents. *Proc. Natl Acad. Sci. USA* 111(25), 9247–9252 (2014).

25 Choi H, Lee Y-S, Hwang DW *et al.* Translational radionanomedicine: a clinical perspective. *Eur. J. Nanomed.* 2, 71–84 (2016).

26 Rahmim A, Zaidi H. PET versus SPECT: strengths, limitations and challenges. *Nucl. Med. Commun.* 29(3), 193–207 (2008).

27 Rima W, Sancey L, Aloy MT *et al.* Internalization pathways into cancer cells of gadolinium-based radiosensitizing nanoparticles. *Biomaterials* 34(1), 181–195 (2013).

28 Benezra M, Penate-Medina O, Zanzonico PB *et al.* Multimodal silica nanoparticles are effective cancer-targeted probes in a modal of human melanoma. *J. Clin. Invest.* 121, 2768–2786 (2011).

29 Xie H, Wang ZJ, Bao A *et al.* In vivo PET imaging and biodistribution of radiolabelled gold nanoshells in rats with tumor xenografts. *Int. J. Pharm.* 395, 324–330 (2010).

30 Chang Y, Chang C, Chang T *et al.* Biodistribution, pharmacokinetics and microSPECT/CT imaging of ^{188}Re-BMEDA-liposome in a C26 murine colon carcinoma solid tumor animal model. *Anticancer Res.* 27, 2217–2226 (2007).

31 Zhou M, Li J, Liang S *et al.* CuS nanodots with ultrahigh efficient renal clearance for positron emission tomography imaging and image-guided photothermal therapy. *ACS Nano* 9(7), 7085–7096 (2015).

32 Mirshojaei SF, Ahmadi A, Morales-Avila E *et al.* Radiolabeled nanoparticles: novel classification of radiopharmaceuticals for molecular imaging of cancer. *J. Drug Target.* 24(2), 91–101 (2016)

33 Popovic Z, Liu W, Chauhan VP *et al.* A nanoparticle size series for in vivo fluorescence imaging. *Angew. Chem. Int. Ed. Engl.* 49(46), 8649–8652 (2010).

34 Arranja AG, Pathak V, Lammers T *et al.* Tumor-targeted nanomedicines for cancer theranostics. *Pharmacol. Res.* 115, 87–95 (2017).

35 Kunjachan S, Pola R, Gremse F *et al.* Passive versus active tumor targeting using RGD- and NGR-modified polymeric nanomedicines. *Nano Lett.* 14, 972–981 (2014).

36 Morlieras J, Dufort S, Sancey L *et al.* Functionalization of small rigid platforms with cyclic RGD peptides for targeting tumors overexpressing $\alpha_v\beta_3$-integrins. *Bioconjugate Chem.* 24(9), 1584–1597 (2013).